THE JOURNAL OF PHYSICAL CHEMISTRY A

Article

pubs.acs.org/JPCA

Gas Phase Kinetics and Equilibrium of Allyl Radical Reactions with NO and NO_2

Matti P. Rissanen,*[,†] Damien Amedro,[‡] Lev Krasnoperov,[§] Paul Marshall,[∥] and Raimo S. Timonen[†]

[†]Laboratory of Physical Chemistry, Department of Chemistry, University of Helsinki, P.O. Box 55 (A.I. Virtasen aukio 1), FIN-00014 Helsinki, Finland

[‡]Laboratoire de Physico-Chimie des Processus de Combustion et de l'Atmosphère CNRS UMR 8522, Université Lille 1, Villeneuve d'Ascq, France

[§]Department of Chemistry and Environmental Science, New Jersey Institute of Technology, University Heights, Newark, New Jersey 07102, United States

[∥]Department of Chemistry and Center for Advanced Scientific Computation and Modeling, University of North Texas, P.O. Box 305070, Denton, Texas 76203, United States

Supporting Information

ABSTRACT: Allyl radical reactions with NO and NO_2 were studied in direct, time-resolved experiments in a temperature controlled tubular flow reactor connected to a laser photolysis/photoionization mass spectrometer (LP-PIMS). In the C_3H_5 + NO reaction 1, a dependence on the bath gas density was observed in the determined rate coefficients and pressure falloff parametrizations were performed. The obtained rate coefficients vary between 0.30−14.2 × 10^{-12} cm^3 s^{-1} (T = 188−363 K, p = 0.39−23.78 Torr He) and possess a negative temperature dependence. The rate coefficients of the C_3H_5 + NO_2 reaction 2 did not show a dependence on the bath gas density in the range used (p = 0.47−3.38 Torr, T = 201−363 K), and they can be expressed as a function of temperature with $k(C_3H_5 + NO_2)$ = (3.97 ± 0.84) × 10^{-11} × (T/300 K) $^{-1.55\pm0.05}$ cm^3 s^{-1}. In the C_3H_5 + NO reaction, above 410 K the observed C_3H_5 radical signal did not decay to the signal background, indicating equilibrium between C_3H_5 + NO and C_3H_5NO. This allowed the C_3H_5 + NO ⇄ C_3H_5NO equilibrium to be studied and the equilibrium constants of the reaction between 414 and 500 K to be determined. With the standard second- and third-law analysis, the enthalpy and entropy of the C_3H_5 + NO ⇄ C_3H_5NO reaction were obtained. Combined with the calculated standard entropy of reaction ($\Delta S°_{298}$ = 137.2 J $mol^{-1}K^{-1}$), the third-law analysis resulted in $\Delta H°_{298}$ = 102.4 ± 3.2 kJ mol^{-1} for the C_3H_5−NO bond dissociation enthalpy.

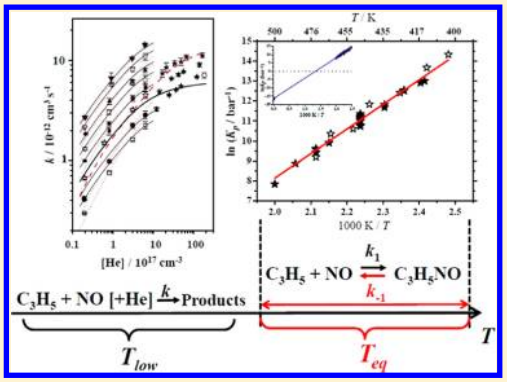

INTRODUCTION

Reactive hydrocarbon free radicals and nitrogen oxides (NO_x = NO + NO_2) are produced in several common environments. Energy released by burning of hydrocarbons creates a variety of reactive intermediates, including unsaturated alkenyl radicals, and combustion under atmospheric conditions leads to the formation of nitrogen oxides.[1,2] Oxides of nitrogen are primary anthropogenic pollutants but also have natural sources in the atmosphere.[3,4] The principles governing mutual reactions of alkenyl radicals and NO_x are important for the understanding of hydrocarbon oxidation mechanisms and optimization of combustion processes.

Allyl radical (C_3H_5) is the simplest conjugated, resonance-stabilized alkenyl radical. Alkenyl radicals are formed in hydrogen abstraction reactions by reactive species (e.g., OH or other radicals) from carbon atoms at the β-position to the double bond in alkenes and by pyrolysis of larger hydrocarbons at elevated temperatures.[5−7] Small unsaturated hydrocarbon radicals with resonance-stabilized structures are thermodynamically more stable than similar saturated radicals lacking resonance stabilization. Consequently, they reach higher concentrations under combustion conditions and play a role in the molecular weight growth chemistry. They are identified as precursors for polycyclic aromatic hydrocarbons (PAHs) and, subsequently, for soot formation.[8−10]

In the present work, two reactions of allyl radical with nitrogen oxides were investigated:

$$C_3H_5 + NO \rightarrow \text{products} \quad (1)$$

$$C_3H_5 + NO_2 \rightarrow \text{products} \quad (2)$$

Both reactions have been studied previously. However, the covered experimental conditions were significantly extended in

Received: August 30, 2012
Revised: January 10, 2013
Published: January 11, 2013

   dx.doi.org/10.1021/jp308621f | J. Phys. Chem. A 2013, 117, 793−805

Table 1. Results and Conditions of the Experiments Used To Measure the Rate Coefficients of the Reaction C_3H_5 + NO → Products[a]

T/K	[He]/10^{16} cm^{-3}	[NO]/10^{13} cm^{-3}	k'_f/s^{-1}	k_{wall}/s^{-1}	k(R+NO)/10^{-12} cm^3 s^{-1}	Δk(R+NO)/10^{-12} cm^3 s^{-1}[b]
CH_2CHCH_2 + NO → Products						
188[c]	2.00	3.14−11.0	89.4−308.6	5	2.69	0.09
188	8.94	0.27−1.05	23.2−79.1	4	6.66	0.83
188[d]	29.5	0.96−2.34	118.2−254.1	9	10.4	0.22
188[d]	62.0	0.76−1.93	98.8−287.7	9	14.2	0.65
201[c]	1.97	2.77−11.1	66.1−236.7	5	2.15	0.07
201	9.18	0.64−1.48	44.7−91.9	5	5.76	0.21
201[d]	30.1	0.89−2.48	96.7−219.7	10	8.11	0.38
201[d]	62.4	0.52−2.08	76.3−232.5	9	10.9	0.75
221[c]	2.10	4.85−9.27	97.6−173.4	3	1.85	0.03
221	8.13	0.63−2.32	20.9−84.0	2	3.90	0.28
221[d]	29.9	1.43−4.85	135.6-311.9	11	6.16	0.34
221[d]	62.1	1.39−3.47	147.5−289.5	11	8.00	0.42
241[c,e]	2.00	9.87−22.6	121.5−306.0	3	1.30	0.04
241	7.89	0.71−2.91	24.7−88.3	2	3.03	0.16
241[d]	30.3	1.16−4.18	113.6−258.7	11	5.96	0.35
241[d]	62.7	1.05−4.08	106.5−256.6	8	6.36	0.66
267[c]	1.99	7.68−15.7	75.5−160.6	3	0.99	0.02
267	7.96	1.41−7.06	53.2−174.4	3	1.98	0.17
267	7.99	1.19−6.22	17.4−145.6	2	2.35	0.07
267[d,e]	30.5	2.08−6.85	126.8−313.2	11	4.18	0.29
267[d]	63.0	1.22−4.26	93.5−224.1	7	5.37	0.49
298	1.98	7.67−30.6	52.4−204.8	4	0.67	0.02
298	6.10	0.53−10.5	10.7−263.2	2	1.50	0.05
298[d]	30.8	2.03−6.02	75.0−199.2	9	3.20	0.09
298[d]	63.4	2.05−6.84	135.1−313.1	9	4.50	0.32
336[c]	1.93	6.80−30.0	30.5−129.2	2	0.42	0.02
336[c]	1.95	6.67−26.3	28.1−114.3	3	0.41	0.01
336[c]	8.08	4.12−13.0	47.5−138.5	5	0.98	0.03
336[d,e]	30.7	2.82−8.38	93.2−196.9	12	2.24	0.13
336[d,e]	63.2	2.15−5.72	85.9−179.8	8	2.84	0.26
363[c]	1.97	12.0−57.3	41.5−176.9	6	0.30	0.01
363[c]	8.09	4.45−17.1	35.7−130.9	6	0.75	0.02
363[d,e]	30.7	2.14−10.7	54.8−186.6	9	1.62	0.07
363[d,e]	63.3	2.02−8.22	85.3−198.7	7	2.25	0.19

[a]Range of precursor (1,5-hexadiene) concentrations used: (0.20−1.88) × 10^{13} cm^{-3}. [b]Statistical uncertainties shown are 1σ. [c]Uncoated 16.5 mm i.d. Pyrex reactor. [d]6 mm i.d. and coated with PDMS, otherwise 17 mm and coated with Halocarbon Wax. [e]Estimated initial radical concentration was less than 7 × 10^{10} cm^{-3}, otherwise less than 6 × 10^{11} cm^{-3}. Estimated overall uncertainty in the determined bimolecular rate coefficients is about ±10%.

the present work, and the C_3H_5 + NO reaction was further characterized with quantum chemical computations.

Tulloch et al.[11] have measured the allyl radical reaction with nitric oxide (NO) at temperatures between 295 and 404 K and from 51 to 501 Torr pressure of argon (1 Torr = 133.3 N m^{-2}). Allyl radicals were produced by 193 nm laser photolysis of 1,5-hexadiene and detected with an UV absorption spectroscopy at 223 nm, employing a high-pressure xenon lamp as a light source. Boyd et al.[12] researched the C_3H_5 + NO equilibrium reaction also by means of UV-absorption spectroscopy but using flash photolysis of 1,5-hexadiene for C_3H_5 radical production. A deuterium lamp was used to generate 220 nm radiation for monitoring radical concentrations. Experiments were conducted over a temperature range of 403 to 473 K and at atmospheric pressure of nitrogen (N_2). In addition, the rate coefficient of the C_3H_5 + NO reaction was determined at 403 K.

The C_3H_5 + NO reaction has also been a subject of a computational investigation. Zhang et al.[13] performed a mechanistic study of the reaction in the singlet potential energy surface using quantum chemical calculations at the CCSD(T)/6-311G(d,p)//B3LYP/6-311G(d,p) level. The experimentally observed pressure dependence was rationalized by relatively stable adduct formation in the entrance channel that cannot isomerize or dissociate further to other products than the original reactants.

The C_3H_5 + NO_2 reaction has only been explored by Slagle et al.[14] at 1 Torr pressure (He) and 300 K temperature. Infrared multiphoton dissociation of allyl bromide was used for C_3H_5 production, and a similar photoionization mass spectrometer as in the current work was employed for real-time monitoring of the decaying radical concentrations.

The aim of the present investigation was to extend the temperature and pressure dependences of the rate coefficients of reactions 1 and 2 studied so far and to characterize the C_3H_5 + NO reaction potential energy surface as well as to provide an accurate measure of the C−N bond energy in C_3H_5−NO.

EXPERIMENTAL SECTION

The flow reactor with laser photolysis coupled to the resonance gas lamp photoionization mass spectrometer (LP-RPIMS) used in this work has been described previously,[15,16] and only a brief

dx.doi.org/10.1021/jp308621f | J. Phys. Chem. A 2013, 117, 793−805

summary of the apparatus and procedures are given here. Reactions were studied in a temperature controlled tubular flow reactor [6 or 17 mm i.d. stainless steel tube coated with Halocarbon wax (HW) or polydimethylsiloxane (PDMS) or a 16.5 mm i.d. uncoated Pyrex tube] coupled to an unfocused ArF exciplex laser photolysis (193 nm) along the reactor. The laser was operated at 3 to 5 Hz repetition depending on the velocity of the gas flow to ensure complete replenishment of the gas mixture between the laser pulses.

Two different photolytic sources were used to generate allyl radicals (C_3H_5), allyl bromide (CH_2CHCH_2Br), and 1,5-hexadiene ($CH_2CHCH_2CH_2CHCH_2$, C_6H_{10}). For allyl bromide, the photolysis products observed (193 nm) were C_3H_5 radicals and Br atoms:

$$CH_2CHCH_2Br + h\nu\ (193\ nm) \rightarrow CH_2CHCH_2 + Br \quad (3)$$

For 1,5-hexadiene there are several possible dissociation channels open at 193 nm, and they have been previously characterized by Morgan et al.,[17] Tulloch et al.,[11] and most recently by Selby et al.[10] The main photolysis channel leads to C3−C4 bond fission, but in addition other products are formed:

$$CH_2CHCH_2CH_2CHCH_2 + h\nu\ (193\ nm) \rightarrow 2CH_2CHCH_2 \quad (4a)$$

$$\rightarrow \text{other products} \quad (4b)$$

The photolysis channel 4b also produces[10,11] allene (C_3H_4), propene (C_3H_6), propane (C_3H_8), cyclopropenylidene (C_3H_2), ethylene (C_2H_4), ethane (C_2H_6), 1,3-butadiene (C_4H_6), butene (C_4H_8), vinylacetylene (C_4H_4), 1,5-hexadiene (C_6H_{10}), C_5H_7, C_4H_7, vinyl (C_2H_3), and methyl (CH_3) radicals. However, allyl radical accounts for more than 80% of all the radical products at this wavelength.[10] As the sensitivity of the apparatus to C_3H_5 is excellent,[18] low precursor concentrations were used (Tables 1, 3, and 5), and photolytical-production of species other than allyl radicals is negligible in comparison with the NO and NO_2 concentrations used. The initial radical concentrations were estimated from the gas flow rates, 1,5-hexadiene concentration, the laser fluences, and the absorption cross section at 193 nm ($\sigma_{193\ nm}$(1,5-hexadiene) = (4.1 ± 0.5) × 10^{-18} cm^2 $molecule^{-1}$).[19] For C_3H_5Br precursor these parameters were not available, and the initial allyl concentrations were estimated from the precursor photodecomposition signal. Initial radical concentrations were estimated to be close to 2 × 10^{11} cm^{-3} in most of the measurements and in the range 3 × 10^{10} cm^{-3} < $[C_3H_5]_0$ < 1 × 10^{12} cm^{-3} in all measurements. Using photolysis of allyl bromide as a C_3H_5 radical source leads to higher background signals, and, hence, 1,5-hexadiene was used in most of the measurements. Nevertheless, allyl bromide was used in some of the equilibrium measurements for comparison.

Selective ionization of the radicals and products was achieved using resonance gas discharge lamps by combining a specific lamp gas with a suitable window filter material. In the study of the kinetics and equilibrium of the C_3H_5 + NO reaction, the C_3H_5 decay signals were measured using a Xe-lamp with a sapphire window producing photons with energy of 8.44 eV. In seeking the products, also Cl- (9.1 eV), H- (10.2 eV), and Ne-lamps (16.9 eV) with CaF_2, MgF_2, and CHS (collimated hole structure plate) filters, respectively, were applied. In the study of the C_3H_5 + NO_2 reaction, the C_3H_5 radical decays were measured with a Cl-lamp using a CaF_2 window (9.1 eV).

At the beginning and at the end of each set of experiments, the C_3H_5 loss rate in the reactor was measured without added reactant (NO or NO_2). The C_3H_5 loss rate (k_{wall}) obtained this way corresponds to all the other loss processes of the radical in the system, except of the C_3H_5 + X (X = NO or NO_2) reaction under investigation. The k_{wall} is the background C_3H_5 loss rate; the starting point ([Reactant] = 0) for the bimolecular plot (see Figures 1 and 5). In the equilibrium measurements, slightly

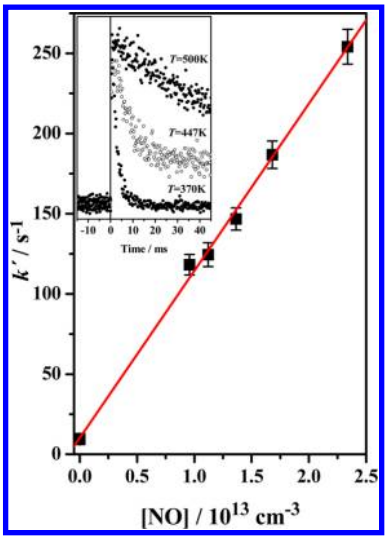

Figure 1. Plot of the pseudo-first-order rate coefficients (k') as a function of NO concentration used to determine the bimolecular rate coefficient of the C_3H_5 + NO reaction at 188 K and 5.75 Torr He ([He] = 2.95 × 10^{17} cm^{-3}). An unweighted fit through the data resulted in the following: $k(C_3H_5 + NO)$ = (1.04 ± 0.22) × 10^{-11} cm^3 s^{-1}, with a wall loss rate of k_{wall} = 10.2 ± 2.9 s^{-1}. Shown in the inset are samples of C_3H_5 radical signal profiles observed at different temperatures.

higher initial allyl radical concentrations (≈ 5 × 10^{11} cm^{-3}) were used to improve the quality of the observed radical signals which resulted in slightly higher measured "wall loss rates", as allyl radical recombination becomes detectable. Nevertheless, the total allyl radical reaction rate in the reactor without added reactant (NO or NO_2) was never larger than 20 s^{-1} (Tables 1, 3 and 5). After a wall rate measurement, a reactant was added in controlled amounts and the corresponding allyl radical loss rates were measured under the pseudo-first-order conditions ($[R]_0 \ll$ [NO or NO_2]).

When bimolecular kinetics were observed, the radical signals recorded could be described by a single exponential function $[R]_t = [R]_0 \times \exp(-k't) + a_0$, where $[R]_t$ is the radical signal at time t, k' is the pseudo-first-order rate coefficient describing the time dependence of the decaying radical concentration and a_0 is the prephotolysis background signal. The bimolecular rate coefficients k(R + NO) and k(R + NO_2) were obtained from the observed pseudo-first-order rate coefficients (k') according to a linear equation $k' = k(R + X) \times [X] + k_{wall}$ by plotting them against corresponding reactant concentrations [X] (X = NO or NO_2) (Figure 1 and 5). In this equation, k_{wall} is the loss rate of the radicals in the reactor without added reactant X, k' is the rate coefficient obtained from the single exponential fitting, [X] is the reactant (NO or NO_2) concentration and k(R + X), the slope of the plot is the bimolecular rate coefficient of the studied reaction.

An expression $k = k_{300K}(T/\ 300\ K)^{-n}$ was fit to the temperature dependence observed in the C_3H_5 + NO_2 reaction rate

dx.doi.org/10.1021/jp308621f | J. Phys. Chem. A 2013, 117, 793−805

Table 2. The C_3H_5 + NO Falloff Fit Parameters Determined with Different Fitting Approaches[f]

	$k_0/10^{-29}$ cm^6 molecule^{-2} s^{-1}[a]	$k_\infty/10^{-12}$ cm^3 molecule^{-1} s^{-1}[a]	n[a]	m[a]
NASA/JPL[b]	6.03 ± 1.32	5.86 ± 0.66	2.98 ± 0.57	2.65 ± 0.30
	(2.46 ± 0.27)	(13.9 ± 0.63)	(4.64 ± 0.43)	(0.82 ± 0.23)
IUPAC[c]	10.5 ± 2.82	7.48 ± 1.10	3.03 ± 0.70	2.62 ± 0.39
	(4.56 ± 0.55)	(16.9 ± 0.88)	(4.47 ± 0.51)	(0.97 ± 0.28)
free F_c[d]	7.49 ± 4.05	6.52 ± 1.62	3.00 ± 0.63	2.64 ± 0.34
	(4.59 ± 2.49)	(16.9 ± 2.75)	(4.48 ± 0.51)	(0.98 ± 0.32)
Tulloch at 296 K[e]	4.0 ± 1.7	13.5 ± 0.30	-	-
Tulloch at 350 K[e]	2.5 ± 1.0	11.2 ± 0.40	-	-
Tulloch at 404 K[e]	1.6 ± 0.6	9.30 ± 0.30	-	-

[a]Uncertainties correspond to statistical 1σ. [b]F_c = 0.6 and denominator in eq E2 is set equal to unity. [c]F_c = 0.4. [d]Obtained with floating F_c; including Tulloch et al.[11] values at 296 K resulted in F_c = (0.40 ± 0.13) and without them the fit returned F_c = (0.51 ± 0.18). [e]Previous results of Tulloch et al.[11] [f]Values in parentheses include the results of Tulloch et al.[11] at 296 K.

coefficients. In addition to the temperature dependence, also a dependence on pressure was observed in the C_3H_5 + NO reaction and the pressure falloff parametrizations of the rate coefficients[20,21] were performed using eqs E1 and E2:

$$k = \frac{k_0 \times \left(\frac{T}{300\text{K}}\right)^{-n}[M]}{1 + \left(\frac{k_0 \times \left(\frac{T}{300\text{K}}\right)^{-n}}{k_\infty \times \left(\frac{T}{300\text{K}}\right)^{-m}}[M]\right)} \times F_c^{\,g} \quad \text{(E1)}$$

$$g = \left[1 + \left(\log \frac{\left(\frac{k_0 \times \left(\frac{T}{300\text{K}}\right)^{-n}[M]}{k_\infty \times \left(\frac{T}{300\text{K}}\right)^{-m}}\right)}{(0.75 - 1.27 \times \log F_c)}\right)^2\right]^{-1} \quad \text{(E2)}$$

where k_0 and k_∞ are the limiting low and high pressure rate coefficients, n and m are their temperature dependences, respectively, and F_c is the center broadening factor that was introduced by Troe[20] to account for the transition regime between the two limiting cases.

At higher temperatures (414 to 500 K), the observed C_3H_5 decay signals did not return to the prephotolysis baseline in the course of reaction, indicating an equilibrium mechanism, and, hence, a different fitting routine was applied. The equilibrium constants ($K_c = k_7/k_{-7}$) were obtained directly from the observed nonsingle-exponential C_3H_5 decays with a numerical simulation of a chemical reaction model (5−7), and the determined K_c values were then converted to K_p (in bar^{-1}). The model used accounted for the wall loss rate (5), the recombination of allyl radicals (6) ($k_5 + k_6 = k_{wall}$; measured separately as explained above), and the reversible reaction with NO (7, −7):

$$C_3H_5 \rightarrow \text{wall} \quad (5)$$

$$C_3H_5 + C_3H_5 \rightarrow C_6H_{10} \quad (6)$$

$$C_3H_5 + NO \rightleftarrows C_3H_5NO \quad (7, -7)$$

The thermochemical parameters for the C_3H_5 + NO reaction were determined using the second- and third-law analyses, by plotting the natural logarithm of the obtained equilibrium constants [$\ln(K_p) + f(T)$] against reciprocal temperature ($1/T$) in a modified van't Hoff plot. From the slope ($\Delta H/R$) and the intercept ($\Delta S/R$) of the plot, the enthalpy and entropy of the reaction were determined.[22] The correction to $\ln(K_p)$ by $f(T)$ originates from the temperature dependences of $\Delta H°$ and $\Delta S°$ and was calculated as described below. For the third-law treatment, the entropy of the reaction (y-axis intercept at $1/T = 0$) and the molar heat capacity of the reaction (ΔC_p for the correction term, $f(T)$) were calculated from the thermochemical parameters of the reactants and products. Calculations were performed using density functional theory at B3LYP/6-311G(d,p) using tight optimization criteria and the ultrafine integration grid and employing the Gaussian09 program suite.[23]

The use of NO and NO_2 as reactants in the measurements needs care as potential impurities and/or side reactions can interfere with the measurements of the R + X (X = NO or NO_2) rate coefficients. NO_2 photolysis is a source of singlet oxygen atoms $O(^1D)$ (55% yield at 193 nm, σ_{193} (NO_2) = 2.9 × 10^{-19} cm^{-2})[24] and addition of NO_2 to the reaction system while neglecting its dimerization to N_2O_4 in the preparation of the source bulb gas mixture results in lower calculated reactant concentrations. The independence of the measured rate coefficients on the dimerization and photolysis of NO_2 have been discussed at length previously[25−27] for investigations conducted with the same methods under similar conditions and hence are not repeated here. NO_2 was used as an 8.5% or 17.0% mixture in He (corresponding to about 45% and 57% of the NO_2 as N_2O_4 in the source bulb, respectively[28]) and was stored in and used from a blackened Pyrex bulb.

Nitric oxide (NO) is converted to higher nitrogen oxides in the presence of O_2. The NO source bulb (100%) was prepared by transferring 99.5% purity NO gas to a Pyrex bulb through a heated copper chip catalyst,[29] in order to convert a potential impurity NO_2 to NO. Afterward the purified NO was still further cold distilled in the source bulb's side arm, and in the measurements, NO gas flow was taken from the bulb placed in an acetone ice slush bath (T_{bath} < 210 K) prepared to trap the possible more reactive higher oxides in the source bulb. All the reactant concentrations in the experiments were determined by measuring the rate of pressure increase in a calibrated volume.

The radical precursors, allyl bromide (C_3H_5Br, Fluka, 99%) and 1,5-hexadiene (C_6H_{10}, Aldrich, 99%), were purified prior to use by several freeze−pump−thaw cycles. Nitric oxide (NO, Linde, 99.5%) was used as a pure 100% gas, nitrogen dioxide (NO_2, Merck, 98%) was diluted in helium to produce an 8.5% or 17.0% mixture, and helium bath gas (He, Messer-Griesheim, 99.9996%) was used as supplied.

RESULTS AND DISCUSSION

The results of the kinetic measurements of the C_3H_5 + NO → *products* (T = 188−363 K, p = 0.39−23.78 Torr He) and C_3H_5 + NO_2 → *products* (T = 201−363 K, p = 0.47−3.38 Torr He) reactions and the experimental conditions of the measurements

dx.doi.org/10.1021/jp308621f | J. Phys. Chem. A 2013, 117, 793−805

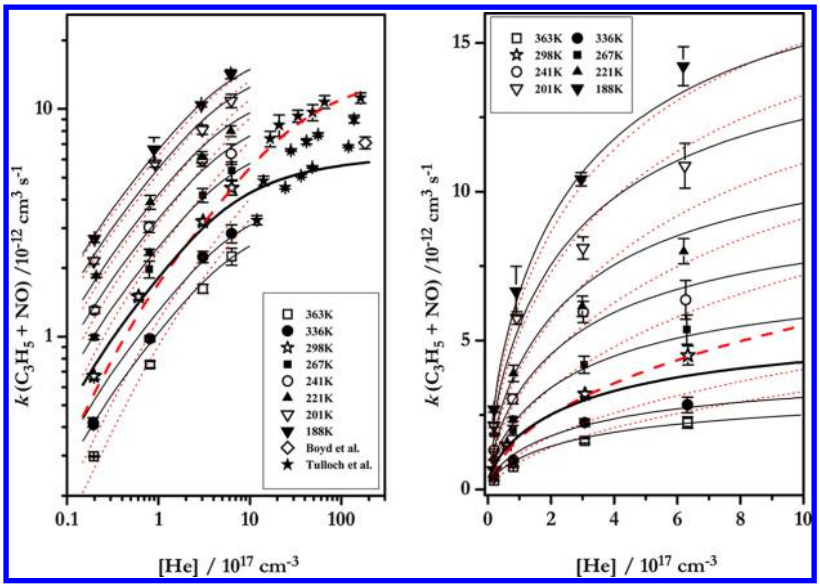

Figure 2. Pressure dependence observed for the rate coefficient of the C_3H_5 + NO reaction presented in logarithmic and linear scales. Shown are the falloff fits obtained with a floating F_c. Fits displayed with dotted lines include the results of Tulloch et al. at 296 K[11] which resulted in F_c = (0.40 ± 0.13); without them the fit returned F_c = (0.51 ± 0.18). The rest of the falloff fit parameters are summarized in Table 2. The thick lines correspond to data at room temperature.

are presented in Tables 1 and 5. The results of the equilibrium measurements of the C_3H_5 + NO ⇄ C_3H_5NO reaction (T = 414−500 K, p = 1.15−2.53 Torr He) are presented in Table 3 together with the conditions of the experiments. The three different sets of experiments are discussed separately.

Possible sources of error in the determination of the rate coefficients and equilibrium constants include reactant concentration over- or underestimation, applicability of the pseudo-first-order approximation, loss of C_3H_5 through competing reactions with photolysis side products, and the possible photochemistry of the used reactants (i.e., photolysis of NO_2) and their influence. In addition, statistical uncertainties of fitting to temporal radical signals affect the overall uncertainty of the determined values.

In general, the determination of the equilibrium constants requires higher quality signals than the determination of bimolecular reaction rate coefficients, if similar accuracy is desired. Hence higher initial radical concentrations were used in the C_3H_5 + NO ⇄ C_3H_5NO equilibrium experiments, and the recombination of allyl radicals (6) was included in the mechanism used to fit the nonsingle-exponential C_3H_5 signals. In the C_3H_5 + NO and C_3H_5 + NO_2 kinetic investigations, lower initial radical concentrations were used. However, even with the higher radical concentrations used the observed "wall loss rates" were in the order of 10−20 s^{-1} (Table 3) and confirm the calculated low initial allyl radical concentrations produced for the experiments ($k(C_3H_5 + C_3H_5)$ = 2.61 × 10^{-11} cm^{-3} s^{-1} by Boyd et al.[12]).

The uncertainty factors, apart from those associated with the measurement routines, are different for each set of experiments: C_3H_5 + NO, C_3H_5 + NO_2, and C_3H_5 + NO ⇄ C_3H_5NO. The largest portion of the estimated overall uncertainty in the determined C_3H_5 + NO_2 rate coefficients (about ±20%) comes from uncertainties in calculated reactant concentrations, whereas, in contrast, the biggest part of the estimated uncertainties in the C_3H_5 + NO ⇄ C_3H_5NO equilibrium constants (about ±20%) results from statistical uncertainties in fitting the temporal radical signals. The determined C_3H_5 + NO rate coefficients do not suffer as much from these uncertainties, as 100% NO was used together with rather low C_3H_5 concentrations, and, hence, the uncertainty is lower, estimated to be about ±10%.

In the study of the kinetics and equilibrium of the C_3H_5 + NO reaction, the C_3H_5 decay signals were measured using an 8.44 eV ionization energy produced by a Xe-lamp with a sapphire window. When a Cl-lamp with a CaF_2 window combination (9.1 eV) was used to ionize C_3H_5, a signal resembling equilibrium was observed even at low temperatures (T < 400 K). When a lower energy Xe-lamp with a sapphire filter was used instead, no problem with the signal profile was observed, i.e., the signal returned to the prephotolysis background level during the time the reaction was followed (>80 ms). In the C_3H_5 + NO_2 investigation, higher ionization energies were used with no apparent problems in the observed radical signals, and the decays measured using a Xe-lamp with sapphire and CaF_2 filters (8.44 and 9.57 eV, respectively) or a Cl-lamp with a CaF_2 gave similar reaction rates; only the background and the signal intensity increased when higher ionization energies were used.

Potential products of the studied reactions were sought with different ionization energies (8.44, 9.1, 10.2, and 16.9 eV), by recording signals at mass numbers of possible products in the absence and presence of excess NO or NO_2. In the C_3H_5 + NO reaction, only a C_3H_5 signal from reaction −7 was observed. In the C_3H_5 + NO_2 reaction, signals of C_3H_5O and C_3H_4O were identified and are discussed below.

C_3H_5 + NO

The bimolecular rate coefficient obtained for the C_3H_5 + NO reaction exhibits a strong negative temperature dependence and a typical pressure dependence of an R + NO association reaction. Below 370 K the measured C_3H_5 signals displayed single exponential decay profiles, and the radical signals were observed to decay back to the level of the prephotolysis background. In this temperature range (188 to 363 K), bimolecular kinetics were observed, and the decay signals could be fitted with a single exponential function ($[R]_t = [R]_0 \times \exp(-k't) + a_0$). Above 414 K the C_3H_5 radical signals displayed a nonsingle-exponential decay profiles and did not decay to the signal

dx.doi.org/10.1021/jp308621f | J. Phys. Chem. A 2013, 117, 793−805

Table 3. Results and Conditions of the Experiments Used To Measure the Equilibrium Constant of the reaction $C_3H_5 + NO \rightleftarrows C_3H_5NO$[a]

T/K	p/Torr[b]	[He]/10^{16} cm^{-3}	[NO]/10^{14} cm^{-3}	[C_3H_5]$_0$/10^{11} cm^{-3}	k_{wall}/s^{-1}	k_7/10^{-13} cm^3 s^{-1}	k_{-7}/s^{-1}	K_c/10^{-15} cm^3	ln(K_p/bar^{-1})[c]	correction $f(T)$[d]
414	2.06	4.80	10.75	4.06	14	2.16	8.5	25.6	13.011	0.034
416	2.06	4.78	5.047	4.08	14	2.91	12.5	23.4	12.916	0.034
424	2.15	4.90	3.972	3.51	13	2.41	14.8	16.4	12.541	0.037
424	2.15	4.90	7.880	3.51	13	2.61	16.3	16.0	12.518	0.037
434	2.22	4.94	5.432	2.87	17	2.25	31.7	7.09	11.680	0.039
434	2.22	4.94	10.40	2.87	17	2.29	28.4	8.06	11.810	0.039
447[e]	1.15	2.48	6.826	4.00	15	1.19	26.6	4.46	11.189	0.043
447[e]	1.15	2.48	11.18	4.00	15	1.38	26.1	5.28	11.357	0.043
447[f]	1.16	2.51	6.143	3.0	20	1.15	40.5	2.85	10.741	0.043
447[f]	1.16	2.51	11.95	3.0	20	1.49	37.2	4.01	11.082	0.043
447[g]	2.31	4.99	5.598	6.21	12	1.83	42.3	4.33	11.159	0.043
447[g]	2.31	4.99	10.78	6.21	12	1.99	41.5	4.81	11.263	0.043
447[f]	2.32	5.01	5.184	1.5	20	2.45	81.9	3.00	10.790	0.043
447[f]	2.32	5.01	10.15	1.5	20	2.44	65.2	3.73	11.010	0.043
465	2.53	5.25	12.24	2.97	15	1.55	119.6	1.29	9.911	0.048
473	2.47	5.04	2.855	5.33	19	2.30	236.5	0.97	9.611	0.051
473	2.47	5.04	5.039	5.33	19	0.86	90.9	0.95	9.583	0.051
473	2.47	5.04	9.739	5.33	19	0.49	60.4	0.82	9.434	0.051
486	2.47	4.91	11.40	2.65	14	2.02	424.0	0.48	8.866	0.055
500	2.52	4.87	11.11	1.90	15	1.55	887.4	0.17	7.834	0.059

[a]Range of precursor concentrations used: (0.94−2.23) × 10^{13} cm^{-3} for C_6H_{10} and (0.95−1.0) × 10^{13} cm^{-3} for CH_2CHCH_2Br. [b]1 Torr = 133.3 N m^{-2}. [c]Estimated overall uncertainty in the determined equilibrium constants is about ±20%. [d]Correction to measured ln(K_p) values as explained in the text. [e]High precursor concentration and low laser power. [f]Precursor CH_2CHCH_2Br. [g]Low precursor concentration and high laser power. Reactor i.d. Seventeen mm and coated with PDMS.

background level. This behavior indicates an equilibrium mechanism in the C_3H_5 + NO reaction above 414 K and is dealt with separately below.

The observed pressure dependence in the rate coefficients can be expressed with pressure falloff curves as described by Troe.[20,21] There are different approaches for fitting falloff curves; either follow expert panel recommendations (NASA/JPL,[30] IUPAC[31]) or perform an unconstrained fit to the experimental data for all the five parameters (k_0, k_∞, n, m, and F_c) in eqs E1 and E2. IUPAC[31] generally uses this latter approach, requiring that the fitted F_c does not deviate too much from the theoretically derived value given by Troe.[21,32] The theoretical F_c value for the present case is 0.4, and it is determined based on the rotational degrees of freedom[21] of the C_3H_5 + NO system. The NASA/JPL panel[30] chooses F_c = 0.6 regardless of the degrees of freedom of the system under study and sets the denominator in eq E2, [0.75 − 1.27 × log(F_c)], equal to unity. All of these parametrizations were fitted to the current experimental C_3H_5 + NO reaction rate coefficients, and the resulting parameters are summarized in Table 2.

The C_3H_5 + NO kinetics have been studied previously by Tulloch et al.[11] and Boyd et al.[12] Tulloch et al.[11] investigated the reaction at 296 to 404 K temperatures and between 50 to 501 Torr pressure of argon (Ar). They used 193 nm photolysis of 1,5-hexadiene to produce allyl radicals for the measurements and UV-absorption at 223 nm generated by a high pressure Xe-lamp for detection. End product analysis was carried out by gas chromatography with flame ionization detection. Tulloch et al.[11] reported a strong pressure dependence with a negative temperature dependence in the obtained bimolecular rate coefficients, which are well reproduced in the current study. Both dependences are also extended in the current investigation with the exception that the bath gas used is He, which is a little more inefficient third body than Ar used by Tulloch. The results obtained here agree well with the rate coefficients of Tulloch et al.[11] (see Figure 2). The temperature dependence determined in this study seems to be slightly stronger than that determined by Tulloch and co-workers,[11] but it is difficult to quantify because of the observed pressure dependence and different third body efficiencies of the bath gases used, and, in addition, because the experimental conditions of the two investigations do not overlap. It is worth noting that the differences between the two results are small and the overall agreement is good.

The current determined C_3H_5 + NO rate coefficients at 298 K extend the results of Tulloch et al.[11] to lower pressures. To exploit this, two different fits were made for each different parametrization: one with the present data only and one that includes the rate coefficients of Tulloch et al.[11] at 296 K. The values obtained for the falloff parameters change significantly when Tulloch et al.[11] results are included in the falloff fits (Table 2 and Figure 2). The fitted low-pressure limiting rate coefficient (k_0) decreases and the power parameter of its temperature dependence (n) increases roughly 50%, while the high-pressure limiting rate coefficient (k_∞) increases and its temperature dependence decreases to about one-third of the value fitted with the current low pressure data only. This indicates a wider falloff range than the current results suggest. It would have been interesting to determine the C_3H_5 + NO rate coefficients at still higher pressures, closer to the experimental conditions used by Tulloch and co-workers.[11] Unfortunately the current experimental setup did not allow pressures much higher than 20 Torr, and hence this goal could not be achieved.

The high- and low-pressure limiting rate coefficients determined by Tulloch et al.[11] are included in Table 2. The agreement between the independently determined values is acceptable. We note that the full data set results in a fitted center broadening factor of F_c = (0.40 ± 0.13), in accordance

dx.doi.org/10.1021/jp308621f | J. Phys. Chem. A 2013, 117, 793−805

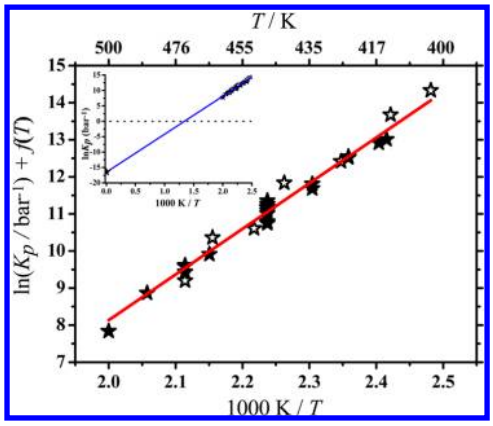

Figure 3. Modified van't Hoff plot of $\ln(K_p/\text{bar}^{-1}) + f(T)$ against $1/T$ used to determine the thermochemistry of the C_3H_5 + NO ⇄ C_3H_5NO reaction. Shown is a linear least-squares fit to the data corresponding to a thermodynamic second-law determination. In the inset the corresponding third-law plot is displayed with a calculated intercept (−137.2 J mol^{-1} K^{-1}/8.31447 J mol^{-1} K^{-1} = −16.50). Current data are indicated by solid symbols. Included are the previous results by Boyd et al.[12] shown with hollow stars.

with the theoretical prediction.[21] Considering only the present results, the fit returned: F_c = (0.51 ± 0.18). It must be emphasized still that the bath gases used in these two studies were different, and so the agreement of the values can be a little fortuitous. Nevertheless, the values determined agree well, and even the rate coefficients at higher temperatures (i.e., 336 to 363 K in the current study and 350 to 404 K in the Tulloch study), experiments that do not have a common temperature between the two studies, seem to concur.

Boyd et al.[12] investigated the C_3H_5 + NO kinetics with the flash photolysis/UV-absorption method at atmospheric pressure of N_2 and at 403 K using 1,5-hexadiene as a photolytic precursor. They determined the rate coefficient $k(C_3H_5 + NO)$ = 7.1 ± 0.4 × 10^{-12} cm^3 s^{-1} which agrees well with the rate coefficients determined in this study, albeit the experimental conditions and the bath gases used are different in the two determinations. The rate coefficient of Boyd et al.[12] is in accordance with the high pressure limit rate coefficients determined in this investigation (Table 2); only the NASA/JPL[30] parametrized fit results in k_∞ that is outside of the combined 1σ uncertainty limits.

The C_3H_5 + NO reaction has also been studied computationally by Zhang et al.[13] at the CCSD(T)/6-311G(d,p)//B3LYP/6-311G(d,p) level. The calculations were stated to reproduce the experimentally observed strong pressure dependence, rationalized by relatively stable adduct formation in the entrance channel that cannot isomerize or dissociate further to other products than the original reactants. The reaction was studied only in its singlet potential energy surface, and no reason was given as to why the reactions triplet surface was not investigated.

The qualitative behavior of the C_3H_5 + NO reaction may be compared to that of the smallest resonantly stabilized hydrocarbon radicals' reaction with nitric oxide; C_3H_3 + NO was investigated by DeSain et al.[33] The C_3H_3 + NO rate coefficients were measured at three temperatures, 195 K, 296 K, and 473 K, and at 2 to 100 Torr pressure of He using a color center laser infrared kinetic spectroscopy. The rate coefficients were observed to vary between 1.1 × 10^{-12} and 1.5 × 10^{-11} cm^3 s^{-1}, in comparison with 3.0 × 10^{-13} to 1.4 × 10^{-11} cm^3 s^{-1} determined for the C_3H_5 + NO rate coefficients in the present study (p = 0.47−3.38 Torr, T = 201−363 K). DeSain et al.[33] observed a strong dependence on bath gas pressure at 195 and 296 K and a negative temperature dependence of the rate coefficients through the temperature range used. According to their calculations, equilibrium between C_3H_3 + NO and C_3H_3NO should be reached at about 500 to 650 K range, which was stated inaccessible due to experimental difficulties. The two closely related reactions, C_3H_3 + NO and C_3H_5 + NO, have very similar dependences on experimental conditions.

$$C_3H_5 + NO \rightleftarrows C_3H_5NO$$

Above 414 K, the recorded C_3H_5 decays did not return to the prephotolysis background level of the signal (Figure 1), and the decays observed had *nonsingle-exponential profiles*. This indicates equilibrium mechanism in the C_3H_5 + NO reaction above 414 K, and the analysis of the signals was carried out

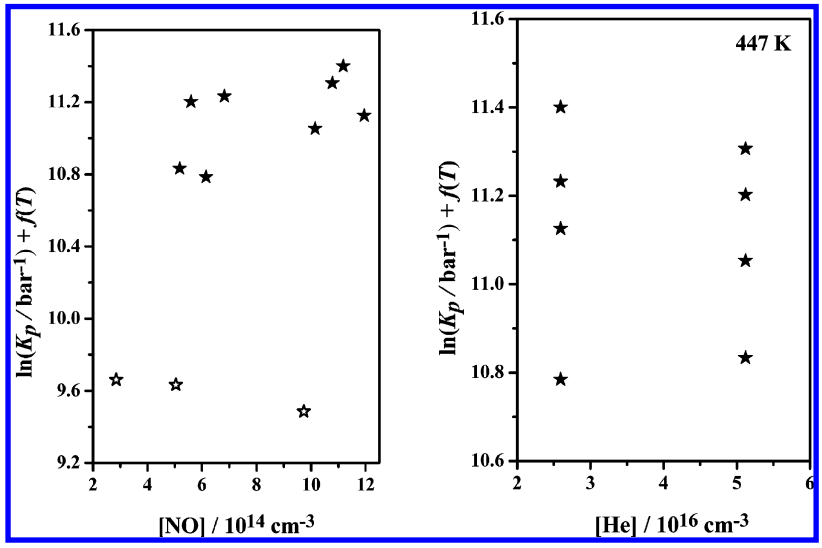

Figure 4. Independence of the determined equilibrium constants of the experimental conditions used: a) $\ln(K_p/\text{bar}^{-1}) + f(T)$ as a function of reactant NO concentrations at T = 447 K (filled stars) and at T = 473 K (hollow stars). b) $\ln(K_p/\text{bar}^{-1}) + f(T)$ as a function of total bath gas densities of the experiments at 447 K.

dx.doi.org/10.1021/jp308621f | J. Phys. Chem. A 2013, 117, 793−805

differently than for the kinetic studies; the signals were fitted with numerical simulations of the reaction mechanism (5−7) described above in the experimental part. The obtained equilibrium constants $K_c = k_7/k_{-7}$ (from which K_p/bar^{-1} is derived) are presented in Table 3 and Figure 3, and their independence of the experimental conditions (NO concentrations and total densities used) is shown in Figure 4.

Thermochemical parameters of the $C_3H_5 + NO \rightleftarrows C_3H_5NO$ reaction were obtained by usual second- and third-law methods by plotting the natural logarithms of the determined equilibrium constants $[\ln(K_p) + f(T)]$ against reciprocal temperature in a modified van't Hoff plot. Here $f(T)$ is a small correction to $\ln(K_p)$ (see below) due to the temperature dependences of ΔH and ΔS and equal to the following: $\Delta C_p/R[(T - 298\ \text{K})/T + \ln(298\ \text{K}/T)]$.[22] ΔC_p was calculated and assumed to be independent of temperature between 414 and 500 K, i.e., in the range the equilibrium measurements were made. The second-law determination, a linear least-squares fit to the data (see Figure 3 and Table 4), resulted in the following: $\Delta H^\circ_{298} = -100.8 \pm 3.0$ kJ mol^{-1} for the enthalpy and $\Delta S^\circ_{298} = -133.6 \pm 6.6$ J mol^{-1} K^{-1} for the entropy of the reaction, with uncertainties given as 1σ of the fit. The third-law determination with the calculated intercept (−137.2 J mol^{-1} K^{-1}/8.31447 J mol^{-1} K^{-1} = −16.50; see below) gave $\Delta H^\circ_{298} = -102.4 \pm 3.2$ kJ mol^{-1} with the error limits given by propagation of errors method when the uncertainties in $\ln(K_p)$ (±20%), estimated uncertainty in ΔS° (±7 J mol^{-1}K^{-1}), and T (±3 K) were taken into account. Accurate estimation of the uncertainty in the calculated entropy of the adduct, C_3H_5NO, at this point, is not feasible. The main contribution comes from the uncertainty of the low frequency vibrations as well as from the rigid rotor - harmonic oscillator approximations used for the six isomers. Simultaneous reduction of all vibrational frequencies by 5% (i.e., multiplication by 0.95) increases the entropy by 2.77 J mol^{-1} K^{-1}. In addition, the maximum entropy difference between the isomers is 3.06 J mol^{-1} K^{-1}. This reflects the scale of the coupling of the moments of inertia. Therefore, it is believed that ±7 J mol^{-1} K^{-1} provides a conservative upper estimate for the uncertainty of the calculated entropy.

The only previous investigation of the $C_3H_5 + NO \rightleftarrows C_3H_5NO$ equilibrium reaction was made by Boyd et al.[12] at atmospheric pressure of N_2 and between 403 to 473 K. They determined $\Delta H^\circ = -112 \pm 5$ kJ mol^{-1} and $\Delta S^\circ = -158 \pm 11$ J mol^{-1} K^{-1} with a second-law treatment. For the third-law determination, the vibrational frequencies of the allyl radical and allyl + NO adduct were estimated using a semiempirical PM3 method, and from these the entropy of the reaction was calculated ($\Delta S^\circ = -150 \pm 7$ J mol^{-1} K^{-1}) giving $\Delta H^\circ = -108 \pm 5$ kJ mol^{-1} for the reaction enthalpy. The correction $f(T)$ to $\ln(K_p)$ was neglected, but it was noted that it has only a minor influence on the entropy and enthalpy values obtained.

The agreement between the equilibrium constants determined in this study and those determined by Boyd et al.[12] is good. Hence the thermochemistry of the reaction was analyzed together with the results of Boyd and co-workers[12] but also according to current results only (Table 4). Combining data from both determinations and using the calculated entropy value (−137.2 ± 7.0 J mol^{-1} K^{-1}) as a fixed point in the fit gave $\Delta H^\circ_{298} = -102.4 \pm 3.2$ kJ mol^{-1} for the third-law enthalpy, with error limits obtained by the propagation of errors method.

$C_3H_5 + NO_2$

The rate coefficients obtained for the $C_3H_5 + NO_2$ reaction possess a negative temperature dependence (T = 201−363 K) and do not depend on the bath gas He pressure within the

Table 4. Current and Previous Values Determined for the Thermochemistry of the Reaction $C_3H_5 + NO \rightleftarrows C_3H_5NO$

study	2nd law ΔH°/kJ mol^{-1}	2nd law ΔS°/J K^{-1} mol^{-1}	3rd law ΔH°/kJ mol^{-1}	calc. ΔS°/J K^{-1} mol^{-1}
Boyd et al.[12]	−112 ± 5	−158 ± 11	−108 ± 5	−150 ± 7[a]
this study $\Delta H_{298}{}^\circ$	−100.8 ± 3.0[b]	−133.6 ± 6.6[b]	−102.4 ± 3.2[c]	−137.2 ± 7.0
combined[d]	−104.9 ± 3.0[b]	−142.6 ± 6.7[b]	−102.4 ± 3.2[c]	−137.2 ± 7.0

[a]Entropy calculated for the third-law plot. [b]Statistical uncertainties shown are one standard error. [c]Uncertainty obtained with the propagation of errors method. [d]Values obtained by fitting the line simultaneously to the current and previous data.[12]

Table 5. Results and Conditions of the Experiments Used To Measure the Rate Coefficients of the Reaction $C_3H_5 + NO_2 \rightarrow$ Products[a]

T/K	[He]/10^{16} cm^{-3}	[NO_2]/10^{12} cm^{-3}	k'_f/s^{-1}	k_{wall}/s^{-1}	k(R+NO_2)/10^{-11} cm^3 s^{-1}	Δk(R+NO_2)/10^{-11} cm^3 s^{-1}[b]
$CH_2CHCH_2 + NO_2 \rightarrow$ Products						
[b] $k(C_3H_5 + NO_2) = (3.97 \pm 0.05) \times 10^{-11} \times (T/300\ \text{K})^{-1.55\pm0.05}$ cm^3 s^{-1}						
201[c]	6.92	1.03−2.73	95.0−215.3	7	7.59	0.25
221[c]	7.0	1.06−2.81	55.3−173.3	1	6.11	0.23
241	6.85	1.65−2.76	73.1−156.2	2	5.56	0.11
266[c]	6.93	1.27−3.73	72.3−176.2	2	4.80	0.27
298[c,d]	1.52	2.98−6.21	136.0−270.2	5	4.00	0.20
298	6.90	1.47−3.82	66.8−161.3	6	4.00	0.05
298[d]	7.78	2.17−5.39	92.7−210.4	7	3.84	0.13
298[c]	10.95	1.37−2.96	58.9−126.0	6	4.26	0.33
336	7.21	1.54−4.10	60.9−134.7	4	3.28	0.13
363	7.21	1.83−3.85	60.3−120.4	5	3.04	0.09

[a]Precursor (1,5-hexadiene) concentrations used: (0.79−3.20) × 10^{12} cm^{-3}. [b]Statistical uncertainties shown are 1σ. [c]Estimated initial radical concentration was less than 6 × 10^{10} cm^{-3}, otherwise less than 1.4 × 10^{11} cm^{-3}. [d]Uncoated 16.5 mm Pyrex reactor, otherwise 17 mm and coated with Halocarbon Wax. Estimated overall uncertainty in the determined bimolecular rate coefficients is about ±20%.

dx.doi.org/10.1021/jp308621f | J. Phys. Chem. A 2013, 117, 793−805

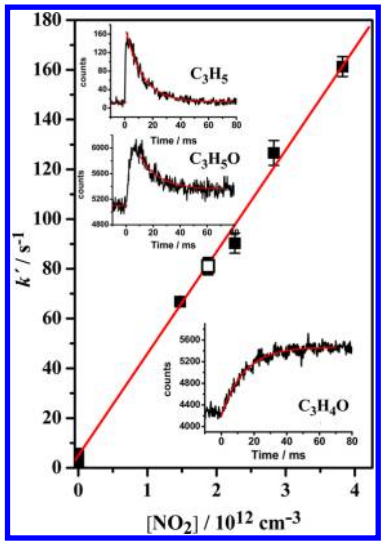

Figure 5. Plot of the pseudo-first-order rate coefficients (k') as a function of reactant concentrations used to obtain the bimolecular rate coefficient of the C_3H_5 + NO_2 reaction at 298 K and 2.13 Torr ([He] = 6.90×10^{16} cm^{-3}). Shown in insets are the C_3H_5 radical decay signal and the C_3H_5O and C_3H_4O product formation signals observed in the measurements. The signals were measured under the conditions of the hollow square in the plot, where [NO_2] = 1.88×10^{12} cm^{-3}. The fits through the signals correspond to the first-order decay and formation coefficients: k'_d (C_3H_5) = (81 ± 3) s^{-1} and k'_f (C_3H_4O) = (68 ± 2) s^{-1} and the decay fit displayed in the C_3H_5O signal was drawn according to the observed C_3H_4O formation kinetics: k'_d (C_3H_5O) = k'_f (C_3H_4O) = 68 s^{-1}. The uncertainties are one standard deviation.

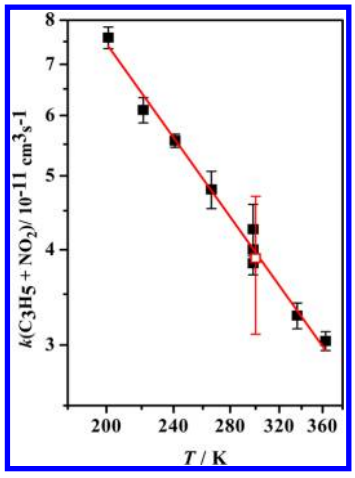

Figure 6. The bimolecular rate coefficients determined for the C_3H_5 + NO_2 reaction shown as a function of temperature. The line through the data corresponds to a fit: $k(C_3H_5 + NO_2) = (3.97 \pm 0.05) \times 10^{-11} \times (T/300\ K)^{-1.55\pm0.05}$ cm^3 s^{-1}, with uncertainties given as 1σ only. Included in the figure is the previous value $k(C_3H_5 + NO_2) = (3.9 \pm 0.8) \times 10^{-11}$ cm^3 s^{-1} determined by Slagle et al.[14] at 300 K and 1 Torr pressure of He shown with an open square.

covered pressure range: p = 0.47−3.38 Torr (Table 5 and Figure 6). The only previous determination of the rate coefficient was made by Slagle et al.[14] at 300 K and 1 Torr pressure of He with infrared multiphoton-induced decomposition of allyl bromide for C_3H_5 production and similar detection method as in the current work. The agreement between the value determined by Slagle et al.[14] ($k_{300K}(C_3H_5 + NO_2) = (3.9 \pm 0.8) \times 10^{-11}$ cm^3 s^{-1}) and the current result ($k_{300K}(C_3H_5 + NO_2) = (4.0 \pm 0.8) \times 10^{-11}$ cm^3 s^{-1}) is excellent (Figure 6).

Products at mass-to-charge ratios (m/z) of 56 and 57 were observed in the C_3H_5 + NO_2 investigation. Slagle et al.[14] also observed formation of products at these mass numbers and identified them as C_3H_4O (m/z = 56) and C_3H_5O (m/z = 57). The kinetics observed for the C_3H_4O formation[14] was stated as too slow to originate from the studied C_3H_5 + NO_2 reaction, indicating secondary chemistry, possibly decomposition or a bimolecular reaction of an allyloxy (C_3H_5O) radical.

The C_3H_5O formation and decay (Figure 5) observed in this study were measured with a H-lamp for ionization (10.2 eV). Slagle et al.[14] were able to ionize this product using a Cl-lamp, which produces considerably lower energy radiation (9.1 eV). When a Cl-lamp was used in the present experiments, only a small signal at a m/z(C_3H_5O) = 57 was detected, too small to deduce the kinetic parameters. When a H-lamp was used instead, a profile corresponding to a radical product was recorded. The radical profile is similar to that recorded by Slagle et al.[14] with the exception that the signal measured in this study does not decay to the prephotolysis background level but instead stays at a constant height *above* the prephotolysis background (Figure 5). This indicates that either another slower formation channel for a product at m/z = 57 and at a lower ionization energy than 10.2 eV is operating or, maybe more likely, that a photodissociation of some formed product (caused by the ionizing light) creates a fragment signal at m/z = 57.

Also the C_3H_4O formation observed in the present study, compared to that observed by Slagle et al.,[14] is different. The formation rate measured here almost matches the C_3H_5 radical decay rate observed in concomitant measurements (Figure 5), while that recorded by Slagle et al.[14] is much too slow to match their measured allyl decay kinetics. In addition, their product signal (C_3H_4O, m/z = 56) has a delayed formation profile. The lamp used in both experiments was a H-lamp. The differences between the two studies are the methods for generating radicals and their precursors: Slagle et al.[14] used multiphoton induced decomposition of allyl bromide for C_3H_5 production, whereas a 193 nm photolysis of 1,5-hexadiene is employed in the current study. The discrepancies between the two product studies are not clear.

The origin of the late product signal observed at m/z = 57 in the current study remains unclear, and the evidence could point to its formation in secondary chemistry. However, low radical concentration (1.5×10^{11} cm^{-3}) was used in this measurement, and furthermore, 1,5-hexadiene photolysis produces only low amounts of other radical species than allyl radicals, and they do not interfere with the C_3H_5 + NO_2 reaction. Based on the signals observed in the current and previous studies, it seems

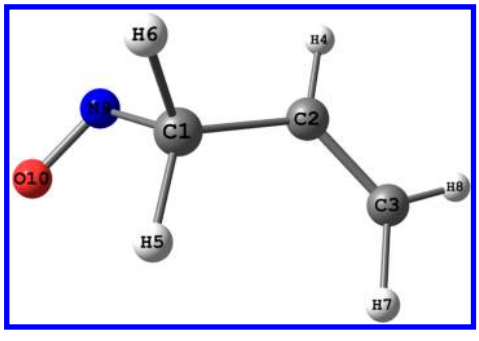

Figure 7. Structure of an example conformation of the allyl + NO adduct.

dx.doi.org/10.1021/jp308621f | J. Phys. Chem. A 2013, 117, 793−805

Table 6. Geometries and the Parameters of the C_3H_5NO Rotamers (A1, B1, and C1) and the Corresponding Optical Isomers (A2, B2, and C2), Allyl Radical, and NO

C_3H_5NO isomer							
A1	A2	B1	B2	C1	C2	C_{2v} allyl	NO
Dihedral Angles D 9−1−2−4 and D 10−9−1−2							
56.4	−56.8	53.7	−53.7	−70.6	70.6		
130.0	−129.8	−3.7	3.7	104.8	−104.8		
Frequencies at B3LYP/6-311G(d,p) Scaled by 0.99							
63.0	63.8	69.0	69.0	60.3	60.3	425.6	1968.9
124.1	125.4	145.4	145.4	85.6	85.6	526.4	
297.1	298.2	252.6	252.6	333.6	333.6	545.8	
416.7	416.6	387.6	387.6	394.3	394.4	777.5	
548.8	548.8	542.2	542.2	552.1	552.1	802.4	
610.8	611.4	741.6	741.6	631.3	631.3	927.2	
819.5	819.3	772.4	772.4	807.1	807.1	1002.8	
925.2	925.4	842.6	842.6	916.7	916.7	1026.6	
942.8	942.8	955.3	955.3	956.4	956.4	1195.5	
952.5	953.3	962.2	962.2	976.7	976.7	1257.5	
1019.0	1019.5	1012.7	1012.7	1019.9	1019.9	1409.2	
1145.2	1145.5	1103.5	1103.6	1127.7	1127.8	1496.1	
1180.8	1181.2	1202.5	1202.5	1219.0	1219.0	1502.1	
1276.4	1277.0	1277.2	1277.2	1265.6	1265.5	3095.6	
1310.8	1310.8	1314.6	1314.6	1312.0	1312.0	3102.2	
1428.0	1428.3	1412.0	1412.0	1431.2	1431.2	3108.5	
1446.9	1447.1	1450.2	1450.2	1452.8	1452.8	3199.3	
1652.3	1652.5	1655.3	1655.3	1642.2	1642.2	3202.1	
1692.2	1692.4	1692.6	1692.6	1686.9	1686.9		
2970.4	2971.6	2975.2	2975.2	3001.7	3001.7		
3052.6	3053.0	3032.8	3032.8	3072.2	3072.2		
3099.8	3100.9	3095.7	3095.7	3100.2	3100.2		
3118.1	3119.6	3126.7	3126.7	3113.1	3113.1		
3184.8	3185.9	3180.3	3180.3	3185.5	3185.5		
Rotational Constants, GHz							
17.227	17.155	13.693	13.694	19.291	19.288	55.089	51.332
2.676	2.681	3.192	3.191	2.663	2.663	10.334	51.332
2.581	2.584	2.800	2.800	2.613	2.613	8.702	0
DFT Energy, atomic units							
247.256800	247.256807	247.256295	247.256295	247.256218	247.256218		
ZPE in kJ mol^{-1}							
199.00	199.08	198.55	198.55	199.40	199.40		
Relative Enthalpy at 0 K in kJ mol^{-1}							
0	0.06	0.88	0.88	1.92	1.92		

most likely that C_3H_5O is produced in the C_3H_5 + NO_2 reaction (possibly from C_3H_5−ONO adduct decomposition) and dissociates by β-scission to give C_3H_4O (acrolein) and H-atom, the reaction C_3H_5 + NO_2 being the rate limiting step. The late signal at m/z = 57 is probably a fragment signal from a formed product, possibly from a C_3H_5−NO_2 or a C_3H_5−ONO adduct, due to photolysis by photoionizing light. Other potential products of the reaction were sought too, but not detected, including the following: C_3H_4, $C_3H_5NO_2$, HONO, and HNO.

In addition, it is of interest to qualitatively compare the results of the two smallest resonantly stabilized hydrocarbon radicals in their reactions with NO_2; C_3H_5 + NO_2 studied in this work and C_3H_3 + NO_2 researched by Geppert et al.[34] at 220 to 336 K and at a few Torr bath gas pressure range using the same apparatus and procedures as in the current study. Geppert et al.[34] determined $k(C_3H_3 + NO_2) = (2.55 \pm 0.05) \times 10^{-11} \times (T/300\ K)^{-1.06\pm0.10}$ $cm^3\ s^{-1}$ for the rate coefficients of the reaction, slightly lower than what is found here for the rate coefficient of the similar C_3H_5 reaction, with also a weaker dependence on temperature ($k(C_3H_5 + NO_2) = (3.97 \pm 0.84) \times 10^{-11} \times (T/300\ K)^{-1.55\pm0.05}$ $cm^3\ s^{-1}$). Geppert et al.[34] observed no pressure dependence of the determined rate coefficients in accordance with the results of this study.

COMPUTATIONS

In addition to the experimental investigation, the behavior of the C_3H_5 + NO reaction was probed also by quantum chemical calculations. The potential energy surface (PES) for the conformations of the C_3H_5NO adduct was explored using density functional theory. B3LYP/6-311G(d,p) calculations were made with the Gaussian09 program,[23] using tight optimization criteria and ultrafine grids for the integrations. A drawing of the allyl + NO adduct is shown in Figure 7, to define the two torsion or dihedral angles d1 = N9−C1−C2−H4, which corresponds to rotation about the C−C bond, and d2 = O10−N9−C1−C2, which corresponds to rotation around the N−C bond. The difference from prior theoretical work[13] is that we account for

dx.doi.org/10.1021/jp308621f | J. Phys. Chem. A 2013, 117, 793−805

different conformations of the C_3H_5NO adduct. Initially a relaxed scan of the PES was conducted as a function of the two torsion angles. This scan revealed 6 minima (3 pairs of optical isomers), which were then optimized separately. Vibrational frequencies for these minima were scaled by a standard factor of 0.99. The geometries are given in the Supporting Information, and the frequencies, moments of inertia, and energies are given in Table 6. A contour map of the hindrance potential for the two internal rotors is shown in Figure 8.

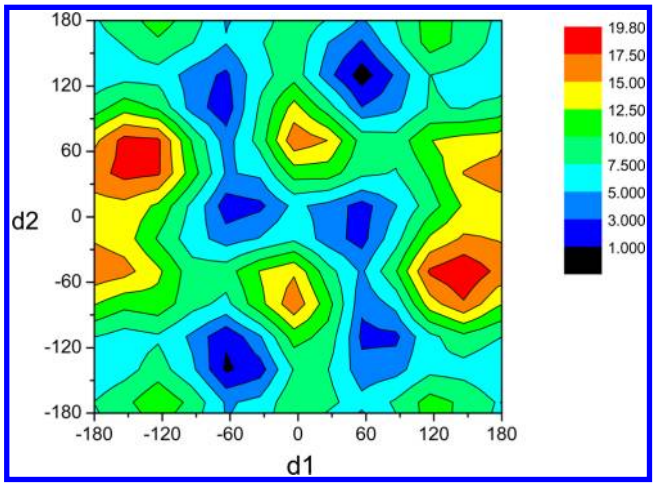

Figure 8. A contour map of the hindrance potential of C_3H_5NO as a function of the dihedral angles d1 (N9−C1−C2−H4) and d2 (O10−N9−C1−C2) in degrees. The energy is in kJ mol^{-1}.

Exact thermochemical calculations for the adduct, allyl nitrosyl, currently are not feasible. There is significant kinematic coupling of the internal rotations with the external rotations via the moments of inertia modulation, as evident from the variation of the rotational constants for external rotations of the rotamers (Table 6). Similar coupling exists also for the two internal rotors. Fortunately, the barriers for the internal rotations (6−12 kJ mol^{-1}) several times exceed the mean thermal energy (RT = 3.3 kJ mol^{-1} at 400 K); therefore, the following approximation is considered to be reasonable. The adduct is treated as an equilibrium mixture of six isomers, three rotamers with corresponding optical isomers (Table 6). The thermodynamic functions for the isomers were calculated using the rigid rotor − harmonic oscillator approximation (with corresponding different rotational constants and vibrational frequencies). The enthalpy and entropy of the equilibrium mixture of the isomers (i.e., of the mixture where equilibrium mole fractions of the isomers were calculated based on their thermochemical parameters) were calculated at different temperatures. The results are listed in Tables 6 and 7.

The calculated entropy of the adduct at 298 K, 331.6 J mol^{-1} K^{-1}, differs significantly from that calculated by Boyd et al. (319 J mol^{-1} K^{-1}),[12] mainly due to the entropy of mixing of the six isomers. The entropy of the allyl radical, 258 J mol^{-1} K^{-1}, is in excellent agreement with the value from Boyd et al.[12] (258 J mol^{-1} K^{-1}). The calculated standard entropy of reaction 7 at 298 K is

$$\Delta S^{\circ}_{298} = -137.2 \text{ J mol}^{-1} \text{ K}^{-1} \quad (8)$$

which was used as the computed intercept (−16.50) in the modified van't Hoff plot, corresponding to the third-law determination (Figure 3).

Calculated entropies and enthalpies were used to calculate the correction $f(T)$ for $\ln(K_p)$ in the modified van't Hoff plot.[22]

$$\ln(K_p) + f(T) = -\Delta H^{\circ}_{298}/RT + \Delta S^{\circ}_{298}/R \quad (9)$$

$$f(T) = (\Delta H^{\circ}_{T} - \Delta H^{\circ}_{298})/RT - (\Delta S^{\circ}_{T} - \Delta S^{\circ}_{298})/R$$

The correction is listed in the last column of Table 7. The correction does not exceed 0.06 in the temperature range of interest, 298 to 500 K, and in this range (and *only* in this range) it can be represented as

$$f(T) = 2.9 \times 10^{-4}(T/\text{K} - 298) \quad (10)$$

CONCLUSIONS

Free radical reactions of allyl with NO and NO_2 were studied in direct measurements and, apart from negative temperature dependence, were observed to display different dependences on the experimental conditions. The C_3H_5 + NO reaction rate coefficient exhibits a strong dependence on pressure for which Troe falloff parametrizations according to different panel recommendations were performed. The fit obtained with a floating center broadening factor and including results from a previous study resulted in F_c = (0.40 ± 0.13), identical to the theory prediction: F_c = 0.4. In contrast, the C_3H_5 + NO_2 reaction rate coefficients showed no dependence on the bath gas density at 298 K and at 0.5 to 3.4 Torr pressure of He. When the temperature was raised to 414 K, an equilibrium was

Table 7. Thermodynamic Functions of the Adduct, C_3H_5NO, and Allyl Radical, C_3H_5, Calculated in This Work[d]

T/K	$S^{\circ}(C_3H_5NO)^a$	$H^{\circ}(C_3H_5NO)^b$	$S^{\circ}(NO)$	$H^{\circ}(NO)$-$H^{\circ}_{298}(NO)$	$S^{\circ}(C_3H_5)$	$H^{\circ}(C_3H_5)$	correction[c]
298.150	331.604	18.283	210.700	0.000	257.994	12.572	0.000
300.000	332.140	18.444	210.900	0.060	258.379	12.687	0.000
350.000	346.279	23.036			268.638	16.020	
400.000	359.824	28.113	219.500	3.040	278.603	19.755	0.025
450.000	372.861	33.652			288.273	23.864	
500.000	385.429	39.620	226.300	6.060	297.641	28.313	0.059
550.000	397.549	45.981			306.702	33.068	
600.000	409.240	52.702	231.900	9.150	315.457	38.101	0.071
650.000	420.519	59.749			323.915	43.386	
700.000	431.404	67.095	236.800	12.310	332.087	48.901	0.077
750.000	441.917	74.715			339.988	54.629	
800.000	452.076	82.587	241.100	15.550	347.633	60.552	0.064

[a]Entropies in J mol^{-1} K^{-1}. [b]Enthalpies in kJ mol^{-1}. [c]Correction $f(T)$ to the $\ln(K_p)$, see text. [d]The thermodynamic functions of nitric oxide, NO, are taken from the literature.[35]

dx.doi.org/10.1021/jp308621f | J. Phys. Chem. A 2013, 117, 793−805

observed between C_3H_5 + NO and C_3H_5NO. Equilibrium constants were determined between 414 and 500 K, and the third-law enthalpy of the reaction was obtained: −102.4 ± 3.2 kJ mol^{-1}, when current and previous determinations were taken into account. Quantum chemical calculations were made to characterize the isomers of the C_3H_5NO adduct.

■ ASSOCIATED CONTENT

Supporting Information

C_3H_5−NO atomic numbers and Cartesian coordinates in 10^{-10} m, derived via B3LYP/6-311G(d,p) theory. This material is available free of charge via the Internet at http://pubs.acs.org.

■ AUTHOR INFORMATION

Corresponding Author

*Phone: +358919150283. E-mail: matti.p.rissanen@helsinki.fi.

Notes

The authors declare no competing financial interest.

■ ACKNOWLEDGMENTS

M.P.R. and R.S.T. appreciate the support from the CMS of CoE of the Academy of Finland. P.M. thanks the R.A. Welch Foundation (Grant B-1174) and the National Science Foundation (Grant CBET-0756144) for support. Computational facilities were purchased in part with NSF Grant CHE-0741936.

■ REFERENCES

(1) Miller, J. A.; Bowman, C. T. Mechanism and Modeling of Nitrogen Chemistry in Combustion. *Prog. Energy Combust. Sci.* **1989**, *15* (4), 287−338.

(2) Warnatz, J.; Maas, U.; Dibble, R. W. *Combustion*, 4th; Springer-Verlag: Berlin, 2006.

(3) Wayne, R. P. *Chemistry of Atmospheres*, 3rd; Oxford University Press, Inc.: New York, U.S.A., 2000.

(4) Jaeglé, L.; Steinberger, L.; Randall, V. M.; Chance, K. Global Partitioning of NO_x Sources Using Satellite Observations: Relative Roles of Fossil Fuel Combustion, Biomass Burning and Soil Emissions. *Faraday Discuss.* **2005**, *130*, 407−423.

(5) Knyazev, V. D.; Slagle, I. R. Thermochemistry and Kinetics of the Reaction of 1-Methylallyl Radicals with Molecular Oxygen. *J. Phys. Chem. A* **1998**, *102*, 8932−8940.

(6) Miller, J. A.; Pilling, M. J.; Troe, J. Unravelling Combustion Mechanisms Through a Quantitative Under- standing of Elementary Reactions. *Proc. Combust. Inst.* **2005**, *30*, 43−88.

(7) Richter, H.; Howard, J. B. Formation of Polycyclic Aromatic Hydrocarbons and Their Growth to Soot—a Review of Chemical Reaction Pathways. *Prog. Energy Combust. Sci.* **2000**, *26*, 565−608.

(8) Miller, J. A.; Melius, C. F. Kinetic and Thermodynamic Issues in the Formation of Aromatic Compounds in Flames of Aliphatic Fuels. *Combust. Flame* **1992**, *91*, 21−39.

(9) Westmoreland, P. R.; Dean, A. M.; Howard, J. B.; Longwell, J. P. Forming Benzene in Flames by Chemically Activated Isomerization. *J. Phys. Chem.* **1989**, *93*, 8171−8180.

(10) Selby, T. M.; Meloni, G.; Goulay, F.; Leone, S. R.; Fahr, A.; Taatjes, C. A.; Osborn, D. L. Synchrotron Photoionization Mass Spectrometry Measurements of Kinetics and Product Formation in the Allyl Radical (H_2CCHCH_2) Self-Reaction. *J. Phys. Chem. A* **2008**, *112*, 9366−9373.

(11) Tulloch, J. M.; Macpherson, M. T.; Morgan, C. A.; Pilling, M. J. Flash Photolysis Studies of Free-Radical Reactions: C_3H_5 + C_3H_5 (293−691 K) and C_3H_5 + NO (295−400 K). *J. Phys. Chem.* **1982**, *86*, 3812−3819.

(12) Boyd, A. A.; Noziere, B.; Lesclaux, R. Kinetics and Thermochemistry of the Reversible Combination Reactions of the Allyl and Benzyl Radicals with NO. *J. Phys. Chem.* **1995**, *99*, 10815−10823.

(13) Zhang, H.; Ding, Y.-H.; Li, Z.-S.; Sun, C.-C. Mechanism of the Radical Reaction Between C_3H_5 and NO. *J. Mol. Struct. (THEOCHEM)* **2006**, *764*, 9−19.

(14) Slagle, I. R.; Yamada, F.; Gutman, D. Kinetics of Free Radicals Produced by Infrared Multiphoton-Induced Decompositions. I. Reactions of Allyl Radicals with Nitrogen Dioxide and Bromine. *J. Am. Chem. Soc.* **1981**, *103*, 149−153.

(15) Eskola, A. J.; Timonen, R. S. Kinetics of the Reactions of Vinyl Radicals with Molecular Oxygen and Chlorine at Temperatures 200−362 K. *Phys. Chem. Chem. Phys.* **2003**, *5*, 2557−2561.

(16) Eskola, A. J.; Wojcik-Pastuszka, D.; Ratajczak, E.; Timonen, R. S. Kinetics of the Reactions of CH_2Br and CH_2I Radicals with Molecular Oxygen at Atmospheric Temperatures. *Phys. Chem. Chem. Phys.* **2006**, *8*, 1416−1424.

(17) Morgan, C. A.; Pilling, M. J.; Tulloch, J. M.; Ruiz, R. P.; Bayes, K. D. Direct Determination of the Equilibrium Constant and Thermodynamic Parameters for the Reaction C_3H_5 + O_2 ⇄ $C_3H_5O_2$. *J. Chem. Soc., Faraday Trans. 2* **1982**, *78*, 1323−1330.

(18) Rissanen, M. P.; Amedro, D.; Eskola, A. J.; Kurten, T.; Timonen, R. S. Kinetic (T = 201−298 K) and Equilibrium (T = 320−420 K) Measurements of the C_3H_5 + O_2 ⇄$C_3H_5O_2$ Reaction. *J. Phys. Chem. A* **2012**, *116*, 3969−3978.

(19) Tonokura, K.; Koshi, M. Absorption Spectrum and Cross Sections of the Allyl Radical Measured Using Cavity Ring-Down Spectroscopy: The Ã ← X Band. *J. Phys. Chem. A* **2000**, *104*, 8456−8461.

(20) Troe, J. Predictive Possibilities of Unimolecular Rate Theory. *J. Phys. Chem.* **1979**, *83*, 114−126.

(21) Troe, J. Toward a Quantitative Analysis of Association Reactions in the Atmosphere. *Chem. Rev.* **2003**, *103*, 4565−4576.

(22) Benson, S. W. *Thermochemical Kinetics*, 2nd ed.; John Wiley & Sons: New York, U.S.A., 1976.

(23) Frisch, M. J.; Trucks, G. W.; Schlegel, H. B.; Scuseria, G. E.; Robb, M. A.; Cheeseman, J. R.; Scalmani, G.; Barone, V.; Mennucci, B.; Petersson, G. A. et al. Gaussian 09, Revision A.1; Gaussian, Inc.: Wallingford, CT, 2009.

(24) Sun, F.; Glass, G. P.; Curl, R. F. The Photolysis of NO_2 at 193 nm. *Chem. Phys. Lett.* **2001**, *337*, 72−78.

(25) Rissanen, M. P.; Eskola, A. J.; Timonen, R. S. Kinetics of the Brominated Alkyl Radical ($CHBr_2$, CH_3CHBr) Reactions with NO2 in the Temperature Range 250−480 K. *Int. J. Chem. Kinet.* **2012**, DOI: 10.1002/kin.20725.

(26) Eskola, A. J.; Geppert, W. D.; Rissanen, M. P.; Timonen, R. S.; Halonen, L. Kinetics of the Reactions of Chlorinated Methyl Radicals (CH_2Cl, $CHCl_2$, and CCl_3) with NO_2 in the Temperature Range 220−360 K. *J. Phys. Chem. A* **2005**, *109*, 5376−5381.

(27) Rissanen, M. P.; Eskola, A. J.; Savina, E.; Timonen, R. S. Kinetics of the Reactions of CH_3CH_2, CH_3CHCl, and CH_3CCl_2 Radicals with NO_2 in the Temperature Range 221−363 K. *J. Phys. Chem. A* **2009**, *113* (9), 1753−1759.

(28) Harwood, M. H.; Jones, R. L. Temperature Dependent Ultraviolet-Visible Absorption Cross Sections of N_2O and N_2O_4: Low-Temperature Measurements of the Equilibrium Constant for $2NO_2$ ⇌ N_2O_4. *J. Geophys. Res.* **1994**, *99* (D11), 22955−22964.

(29) Stahl, Q. R. Method and Apparatus for Converting Nitrogen Dioxide to Nitric Oxide; Springfield, VA, United States Patent 3979501. http://www.freepatentsonline.com/3979501.html (accessed Jan 16, 2013).

(30) Sander, S. P.; Friedl, R. R.; Ravishankara, A. R.; Golden, D. M.; Kolb, C. E.; Kurylo, M. J.; Molina, M. J.; Moortgat, G. K.; Keller-Rudek, H.; Finlayson-Pitts, B. J. et al. *Chemical Kinetics and Photochemical Data for Use in Stratospheric Modelling: Evaluation Number 15*, Publication 06-2; National Aeronautics and Space Administration, Jet Propulsion Laboratory, California Institute of Technology, Pasadena, CA, 2006.

(31) Atkinson, R.; Baulch, D. L.; Cox, R. A.; Crowley, J. N.; Hampson, R. F.; Hynes, R. G.; Jenkin, M. E.; Rossi, M. J.; Troe, J.

Evaluated Kinetic and Photochemical Data for Atmospheric Chemistry: Volume I - Gas Phase Reactions of O_x, HO_x, NO_x and SO_x Species. *Atmos. Chem. Phys.* **2004**, *4*, 1461−1738.
(32) Golden, D. M. Evaluating Data for Atmospheric Models, an Example: CH_3O_2 + NO_2 = $CH_3O_2NO_2$. *Int. J. Chem. Kinet.* **2005**, *37* (10), 625−632.
(33) DeSain, J. D.; Hung, P. Y.; Thompson, R. I.; Glass, G. P.; Scuseria, G.; Curl, R. F. Kinetics of the Reaction of Propargyl Radical with Nitric Oxide. *J. Phys. Chem. A* **2000**, *104*, 3356−3365.
(34) Geppert, W. D.; Eskola, A. J.; Timonen, R. S.; Halonen, L. Kinetics of the Reaction of Vinyl (C_2H_3) and Propargyl (C_3H_3) Radicals with NO_2 in the Temperature Range 220−360 K. *J. Phys. Chem. A* **2004**, *108*, 4232−4238.
(35) Linstrom, P. J.; Mallard, W. G. NIST Chemistry Webbook, NIST Standard Reference Database Number 69, June 2005, National Institute of Standards and Technology: Gaithersburg, MD, 20899. Web address: http://webbook.nist.gov (retrieved in 2.2012).